NLO Analysis of Small-k_{T} Region in Drell-Yan Production with Parton Branching

S. Taheri Monfared⬥*

Deutsches Elektronen-Synchrotron DESY, Germany

E-mail: taheri@mail.desy.de

The Parton-Branching Method (PB) facilitates the determination of Transverse Momentum Dependent (TMD) parton densities across a wide k_{T} range, spanning small to large transverse momentum scales. In the small k_{T} region, both intrinsic parton motion and resummed ultra-soft gluons are significant contributors. Our analysis highlights their crucial role in shaping integrated and TMD parton densities.

Using PB-derived TMD parton densities and a NLO calculation in MC@NLO style, we compute the transverse momentum spectrum of Drell-Yan pairs across a broad mass range. The spectrum's sensitivity to the intrinsic k_{T} distribution allows us to fine-tune parametric parameters. Starting from the PB-NLO-HERAI+II-2018 set2 TMD parton distributions, we determine the intrinsic k_{T} distribution width, resulting in a slightly wider profile than the default set. Importantly, this width remains independent of Drell-Yan pair mass and center-of-mass energy ($\sqrt{s}$), distinguishing our approach.

The European Physical Society Conference on High Energy Physics (EPS-HEP2023)
21-25 August 2023
Hamburg, Germany

---

*Speaker

https://pos.sissa.it/

1. Introduction

The Drell-Yan (DY) lepton pair production in hadron collisions serves as an essential probe of various QCD phenomena. At low transverse momentum (p_{T}) of the DY pair, non-perturbative parton motion within hadrons becomes significant. In this regime, resumming multiple soft gluon emissions is crucial, while at higher p_{T}, perturbative contributions dominate.

Various methods, including CSS, TMD resummation, and parton shower calculations, have been used to describe DY pair transverse momentum spectra across different DY masses (m_{DY}) and center-of-mass energies ($\sqrt{s}$). The Parton Branching (PB) method [1, 2], notably, successfully reproduces these spectra at both LHC and lower energies without parameter adjustments, in contrast to other approaches that necessitate energy-dependent intrinsic k_{T} distributions [3].

Our study delves into the low k_{T} behavior of PB-TMD parton distributions, emphasizing the significance of including very soft gluon emissions following DGLAP. These unresolvable emissions significantly influence inclusive parton distributions, especially in the low-k_{T} TMD spectrum.Our findings reveal that the PB-NLO-HERAI+II-2018 set2 (abbreviated as PB-set2) TMD distributions result in a minor pure intrinsic-k_{T} contribution, as most of the small-k_{T} effects are accounted for within the PB framework.

2. PB TMDs and DY cross section

To investigate various low-p_{T} spectrum contributions across different m_{DY} and $\sqrt{s}$ scenarios, we employ the PB TMD method, as outlined in [4, 5]. This involves extracting NLO hard-scattering matrix elements from MadGraph5_aMC@NLO and matching them with TMD parton distributions and showers derived from PB evolution, using the subtractive matching procedure introduced in [6]. The PB evolution equations for TMD parton distributions $\mathcal{A}_a(x, \mathbf{k}, \mu^2)$ of flavor a are given by:

$$
\begin{aligned}
\mathcal{A}_a(x, \mathbf{k}, \mu^2) &= \Delta_a(\mu^2)\, \mathcal{A}_a(x, \mathbf{k}, \mu_0^2) + \sum_b \int \frac{d^2 \mathbf{q}'}{\pi \mathbf{q}'^2} \frac{\Delta_a(\mu^2)}{\Delta_a(\mathbf{q}'^2)}\, \Theta(\mu^2 - \mathbf{q}'^2)\, \Theta(\mathbf{q}'^2 - \mu_0^2) \\
&\times \int_x^{z_M} \frac{dz}{z}\, P_{ab}^{(R)}(\alpha_s, z)\, \mathcal{A}_b\left(\frac{x}{z}, \mathbf{k} + (1-z)\mathbf{q}', \mathbf{q}'^2\right) \,,
\end{aligned}
\tag{1}
$$

where z_M is the soft-gluon resolution scale [5], and z is the longitudinal momentum transferred at the branching. Δ_a is the Sudakov form factor. This branching evolution fulfills soft-gluon angular ordering and is essential for well-defined TMD distributions.

The distribution $\mathcal{A}_a(x, \mathbf{k}, \mu_0^2)$ at the starting scale μ_0 of the evolution is a nonperturbative boundary condition to the evolution equation, and is to be determined from experimental data. We parameterize it as:

$$
\mathcal{A}_{0,b}(x, k_T^2, \mu_0^2) = f_{0,b}(x, \mu_0^2) \cdot \exp\left(-|k_T^2|/2\sigma^2\right) / (2\pi\sigma^2) \,,
\tag{2}
$$

with $\sigma = q_s/\sqrt{2}$, independent of parton flavor and x, where q_s is the intrinsic-k_T parameter. The scale at which the strong coupling α_s is to be evaluated in Eq. (1) can follow two scenarios, either $\alpha_s(\mathbf{q}'^2)$ or $\alpha_s(q_T^2)$ while $q_T^2 = \mathbf{q}'^2(1-z)^2$. In this study, we focus on the scenario where α_s is

determined as a function of the transverse momentum q_T^2, referred to as PB-set2. This scenario provides a better description of various measurements and utilizes an intrinsic-k_T parameter $q_s = 0.5$ GeV.

3. Non-perturbative contribution

The PB TMD method incorporates Sudakov evolution through phase space integrations of relevant kernels over the resolvable region, encompassing momentum transfers z up to the soft-gluon resolution scale z_M. The effects of z_M on parton distributions and transverse momentum distributions are significant. The choice of z_M mainly affects the soft region, while the perturbative region with $q_t > q_0$ remains unaffected by this choice. A scale like $z_M = z_{\rm dyn} = 1 - q_0/\mu'$ removes emissions with $q_t < q_0$. In contrast, using $z_M \rightarrow 1$ includes very soft emissions by default. The intrinsic-k_T distribution has a more pronounced effect at smaller scales, but its contribution decreases at larger scales. The detailed description of the non-perturbative contribution for PB-set1 and PB-set2 can be found in Ref. [7, 8].

4. DY Cross Section Computation

The cross section for DY production is computed at NLO using the MCatNLO method. In this approach, the collinear and soft contributions from the NLO cross section are subtracted, as they will be included later when applying parton showers or TMD parton densities. We incorporate TMD parton distributions and parton showers into the MCatNLO calculation using CASCADE3 [9], as discussed in detail in Ref. [6]. We utilize the Herwig 6 subtraction terms in MCatNLO, which are consistent with the PB-set TMD parton distribution sets described earlier. The predicted cross sections are calculated using the integrated versions of the NLO parton densities PB-set, along with $\alpha_s(m_Z) = 0.118$ at NLO.

The factorization scale μ for the hard process calculation is set to $\mu = \frac{1}{2} \sum_i \sqrt{m_i^2 + p_{t,i}^2}$, where the sum includes all final state particles. For DY production, this includes all decay leptons and the final jet. When generating transverse momentum according to the PB distributions, μ is set to $\mu = m_{\rm DY}$. In the case of real emission, it is set to $\mu = \frac{1}{2} \sum_i \sqrt{m_i^2 + p_{t,i}^2}$. The generated transverse momentum is constrained by the matching scale μ_m = SCALUP [9]. As there are currently no PB-fragmentation functions available, the final state parton shower in CASCADE3 is generated using Pythia, including photon radiation from the lepton pair.

5. The transverse momentum distribution of Drell-Yan lepton pairs

The transverse momentum spectrum of DY lepton pairs at $\sqrt{s} = 13$TeV has been measured across a wide range of $m_{\rm DY}$ values ($m_{\rm DY} = [50, 76, 106, 170, 350, 1000]$ GeV) by CMS [10]. This measurement is provided including a detailed uncertainty breakdown, including a complete treatement of experimental uncertainties with correlations between bins of the measurement.

We compare these measurements with predictions from MCatNLO+CAS3, utilizing PB-sets. Notably, as previously observed in various studies [6, 11–13], PB-set1 tends to overestimate contributions at low transverse momenta ($p_T(\ell\ell)$), while PB-set2 aligns well with the measurements
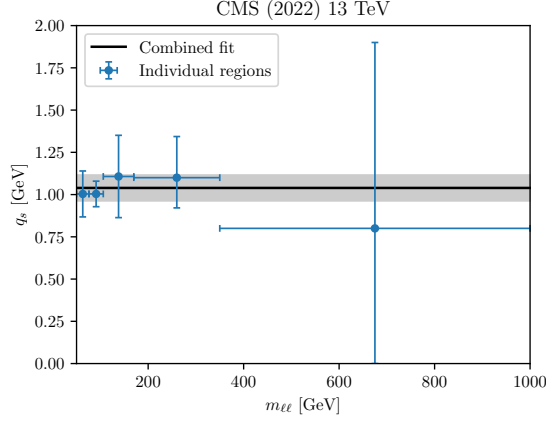
Figure 1: The values of q_s obtained in each m_{DY}-bin as obtained from Ref. [10]. Indicated is also the final value of q_s.

without requiring additional parameter adjustments. Given the success of MCatNLO+CAS3 with PB-set2 in describing the DY $p_T(\ell\ell)$-spectrum in the low $p_T(\ell\ell)$-region, we now explore the significance of the intrinsic-k_T distribution. In PB-sets, this distribution is represented as a Gaussian as shown in Eq. 2. We focus on $p_T(\ell\ell)$ values below the peak region to avoid the absence of higher-order contributions in the matrix element. We use the detailed breakdown of the experimental uncertainties provided on the CMS public website. To determine of the intrinsic-k_T we vary the q_s parameter and calculate a χ^2 to quantify the model agreement with the measurement. Detailed discussion on the treatment of the uncertainties and calculation of χ^2 is available in Ref. [8].

The best fit value, extracted using the correlated uncertainties, is: $q_s = 1.04 \pm 0.03\,(\text{data}) \pm 0.05\,(\text{scan}) \pm 0.05\,(\text{binning})\,\text{GeV}$. This value and its uncertainty are shown as a black line and shaded area in Fig. 1 for comparison with the individual m_{DY} bins. Figure 2 illustrates the variation of q_s as a function of m_{DY} and $\sqrt{s}$, utilizing data from different measurements mentioned in Refs.[10, 14–21]. Notably, the value of $q_s = 1.04 \pm 0.08\,\text{GeV}$, determined from the measurements in Ref.[10], remains applicable across all m_{DY} ranges and for various $\sqrt{s}$ values.

6. Summary and Conclusion

We here apply the PB approach to low k_T DY production, presenting results from the work in Ref. [8]. In this study, we discuss the PB-TMD distributions, focusing on soft and low transverse momenta contributions. We obtain the NLO cross section of the DY process and compare it to recent LHC measurements. We emphasize the importance of the soft, non-perturbative region for both integrated and transverse momentum distributions. The key result of this work is the extraction of the intrinsic-k_T parameter q_s from measured p_T dependence of DY cross sections at various $\sqrt{s}$ and m_{DY}. We find a consistent value of $q_s = 1.04 \pm 0.08$ GeV, independent of m_{DY} and $\sqrt{s}$, in agreement with expectations from Fermi motion in protons. This contrasts with typical Monte Carlo generators that require $\sqrt{s}$ and m_{DY}-dependent widths for intrinsic Gauss distributions. The stability of our obtained q_s value is influenced by the "non-perturbative Sudakov form factor," which is crucial for stable integrated distributions.
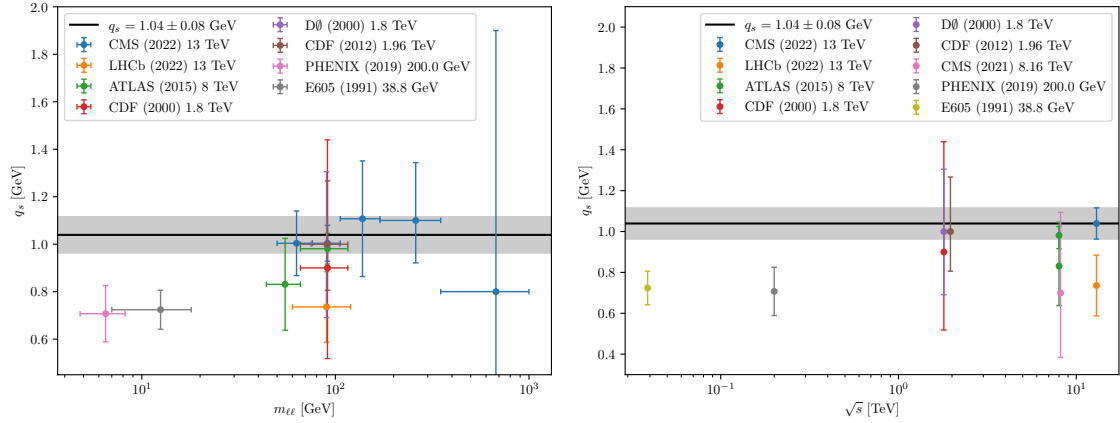
Figure 2: Left: the value of q_s as a function of the DY-mass as obtained from the measurements in Refs. [10, 14–21]. **Right** : same as a function of $\sqrt{s}$.

Acknowledgments

The results discussed in this contribution are based on the work in Ref. [8]. Many thanks to all co-authors for collaboration. I am grateful to the organizers of EPS2023 for the invitation to present these results at the workshop.

References

[1] A. Bermudez Martinez, *et al.*, "Collinear and TMD parton densities from fits to precision DIS measurements in the parton branching method," Phys. Rev. D **99** (2019) no.7, 074008, arXiv:1804.11152.

[2] H. Jung, S. Taheri Monfared and T. Wening, "Determination of collinear and TMD photon densities using the Parton Branching method," Phys. Lett. B **817** (2021), 136299, arXiv:2102.01494.

[3] S. Gieseke, M. H. Seymour, and A. Siodmok, "A Model of non-perturbative gluon emission in an initial state parton shower," *JHEP* **06** (2008) 001, arXiv:0712.1199.

[4] F. Hautmann, *et al.*, "Collinear and TMD quark and gluon densities from Parton Branching solution of QCD evolution equations," *JHEP* **01** (2018) 070, arXiv:1708.03279.

[5] F. Hautmann, *et al.*, "Soft-gluon resolution scale in QCD evolution equations," *Phys. Lett. B* **772** (2017) 446, arXiv:1704.01757.

[6] H. Yang, *et al.*, "Back-to-back azimuthal correlations in Z+jet events at high transverse momentum in the TMD parton branching method at next-to-leading order," *Eur. Phys. J. C* **82** (2022) 755, arXiv:2204.01528.

[7] M. Mendizabal, *et al.*, "On the role of soft gluons in collinear parton densities," arXiv:2309.11802.

[8] I. Bubanja, *et al.*, "The small k_T region in Drell–Yan production at next-to-leading order with the parton branching method," *Eur. Phys. J. C* **84** (2024) no.2, 154, `arXiv:2312.08655`.

[9] S. Baranov, *et al.*, "CASCADE3: A Monte Carlo event generator based on TMDs," *Eur. Phys. J. C* **81** (2021) 425, `arXiv:2101.10221`.

[10] CMS Collaboration, "Measurement of the mass dependence of the transverse momentum of lepton pairs in Drell-Yan production in proton-proton collisions at $\sqrt{s} = 13$ TeV," `arXiv:2205.04897`, `https://cms-results.web.cern.ch/cms-results/public-results/publications/SMP-20-003/index.html`.

[11] M. I. Abdulhamid et al., "Azimuthal correlations of high transverse momentum jets at next-to-leading order in the parton branching method," *Eur. Phys. J. C* **82** (2022) 36, `arXiv:2112.10465`.

[12] A. Bermudez Martinez et al., "The transverse momentum spectrum of low mass Drell–Yan production at next-to-leading order in the parton branching method," *Eur. Phys. J. C* **80** (2020) 598, `arXiv:2001.06488`.

[13] A. Bermudez Martinez, *et al.*, "Production of Z-bosons in the parton branching method," *Phys. Rev. D* **100** (2019) 074027, `arXiv:1906.00919`.

[14] LHCb Collaboration, "Precision measurement of forward Z boson production in proton-proton collisions at $\sqrt{s} = 13$ TeV," *JHEP* **07** (2022) 026, `arXiv:2112.07458`.

[15] CMS Collaboration, "Study of Drell-Yan dimuon production in proton-lead collisions at $\sqrt{s_{NN}} = 8.16$ TeV," *JHEP* **05** (2021) 182, `arXiv:2102.13648`.

[16] ATLAS Collaboration, "Measurement of the transverse momentum and ϕ_η^* distributions of Drell–Yan lepton pairs in proton–proton collisions at $\sqrt{s} = 8$ TeV with the ATLAS detector," *Eur. Phys. J. C* **76** (2016) 291, `arXiv:1512.02192`.

[17] CDF Collaboration, "The transverse momentum and total cross section of e^+e^- pairs in the Z boson region from $p\bar{p}$ collisions at $\sqrt{s} = 1.8$ TeV," *Phys. Rev. Lett.* **84** (2000) 845, `arXiv:hep-ex/0001021`.

[18] D0 Collaboration, "Measurement of the inclusive differential cross section for Z bosons as a function of transverse momentum in $\bar{p}p$ collisions at $\sqrt{s} = 1.8$ TeV," *Phys. Rev. D* **61** (2000) 032004, `arXiv:hep-ex/9907009`.

[19] CDF Collaboration, "Transverse momentum cross section of e^+e^- pairs in the Z-boson region from $p\bar{p}$ collisions at $\sqrt{s} = 1.96$ TeV," *Phys. Rev. D* **86** (2012) 052010, `arXiv:1207.7138`.

[20] PHENIX Collaboration, "Measurements of $\mu\mu$ pairs from open heavy flavor and Drell-Yan in $p + p$ collisions at $\sqrt{s} = 200$ GeV," *Phys. Rev. D* **99** (2019) 072003, `arXiv:1805.02448`.

[21] G. Moreno et al., "Dimuon production in proton - copper collisions at $\sqrt{s} = 38.8$ GeV," *Phys. Rev. D* **43** (1991) 2815.